

Purdue University
Purdue e-Pubs

International Compressor Engineering Conference

School of Mechanical Engineering

1984

Efficiency Improvement in Rotary Compressor

T. Nomura

M. Ohta

K. Takeshita

Y. Ozawa

Follow this and additional works at: <https://docs.lib.purdue.edu/icec>

Nomura, T.; Ohta, M.; Takeshita, K.; and Ozawa, Y., "Efficiency Improvement in Rotary Compressor" (1984). *International Compressor Engineering Conference*. Paper 468.
<https://docs.lib.purdue.edu/icec/468>

This document has been made available through Purdue e-Pubs, a service of the Purdue University Libraries. Please contact epubs@purdue.edu for additional information.

Complete proceedings may be acquired in print and on CD-ROM directly from the Ray W. Herrick Laboratories at <https://engineering.purdue.edu/Herrick/Events/orderlit.html>

EFFICIENCY IMPROVEMENT IN ROTARY COMPRESSOR

Teruo Nomura, Senior Engineer, Nagoya Air-conditioning & Refrigeration Machinery Works, Mitsubishi Heavy Industries, Ltd., Aichi, Japan.

Masaru Ohta, Senior Engineer, Nagoya Technical Institute, Mitsubishi Heavy Industries, Ltd., Nagoya, Japan.

Koji Takeshita and Yutaka Ozawa, Senior Engineers, Takasago Technical Institute, Mitsubishi Heavy Industries, Ltd., Takasago, Japan.

ABSTRACT

This paper presents how we improved the efficiency in rotary compressor. At first, we made effort to estimate the power losses in the compressor, to analyze the operating conditions of the bearing and to calculate the performance of the compressor. Next, the temperature in housing and pressure in cylinder were measured in real compressors in order to obtain the data on the internal conditions of the compressor. As for the points which were insufficient in the measurement with a real compressor, model tests were also conducted using the test apparatus which simulated the conditions of leakage and lubrication in the real compressor. Then, on the basis of the analysis and the measurement above-mentioned, we evaluated the effects of various counter-measures to reduce losses. By employing the most effective counter-measures, we obtained a 12% increase in efficiency and minimized the decrease of efficiency when a capacity control device was in function.

INTRODUCTION

Rotary compressors have been used for room air-conditioners in the Japanese market, because of the compactness, light-weight and high efficiency. Recently we have successfully developed rotary compressors with the highest efficiency, and we commenced marketing room air-conditioners with the rotary compressor. The rotary compressors described in this paper are of the rolling piston type and their typical structure is shown in Fig. 1. Since the fall of 1982, the room air-conditioners produced in Japan are under regulation of the Energy Conservation Act notified in October, 1979. Therefore, their energy efficiency ratio (EER) is required to be within the limited value specified in the Act.

In addition, users want energy saving appliances, as the result of the recent tendency of high price of electricity. Accordingly, the higher efficiency of compressors, which consume most of the power needed for room air-conditioner, is the most important factor in saving energy. As for the heat pump type air-conditioners, large capacity compressors are usually adopted in place of auxiliary electric heaters in order to reduce electric consumption, that is, to improve efficiency. In this case however, it is necessary to control the capacity of the compressor, because less capacity is required for cooling than for heating. In order to meet the needs of the market

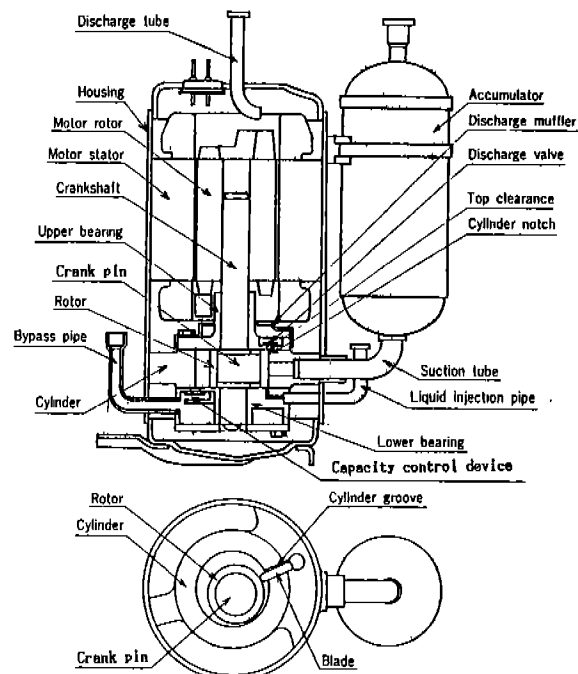


Fig. 1 Sectional Views of Rotary Compressor with Capacity Control Device

stated above, we have developed a high efficiency rotary compressor providing a capacity control function.

METHOD FOR CALCULATING THE LOSS

Indicated Loss

(1) Leakage ... The cylinder part of a rotary compressor is immersed in the oil of the discharged gas pressure in the compressor housing, so that usually the oil is supplied to each leaking clearance. There is, however, some possibility that the compressed refrigerant gas leaks through the clearances. In case the oil leaks, it is considered that the refrigerant dissolved in the oil evaporates in the process that the pressurized oil leaks to the low pressure side, for the solubility of refrigerant differs according to the pressure and temperature. This means the gas leaks with the oil. According to the rotating angle, the pressure difference and the length and width of the flow paths vary. Thus the flow rate is not constant, and the leakage $dG_l/d\varphi$ is given by the following equation.

$$\frac{dG_l}{d\varphi} = \left\{ \begin{array}{l} \frac{A_{eff}}{\omega v} \sqrt{\frac{2gAh}{A}} \left(\begin{array}{l} \text{In case of the leak of} \\ \text{refrigerant gas} \end{array} \right) \\ \frac{4\alpha\gamma bc^3 \Delta p}{12\omega\mu l} \left(\begin{array}{l} \text{In case of the leak of oil with} \\ \text{the dissolved refrigerant} \end{array} \right) \end{array} \right\} \quad (1)$$

where,

- A_{eff} : Effective flow area at leaking clearance
- v : Gas specific volume at leaking clearance
- h : Enthalpy change at leaking clearance
- A : Thermal equivalent of work
- g : Gravity acceleration
- ω : Shaft rotating angular velocity
- $dG_l/d\varphi$: Refrigerant leakage per unit rotating angle
- γ : Specific gravity of solution
- b : Width of leaking clearance
- c : Magnitude of clearance
- l : Length of leaking clearance
- μ : Viscosity of solution
- Δp : Pressure difference
- $\Delta\alpha$: Solubility difference

(2) Suction pressure loss ... The rotary compressor has neither suction valve nor suction cavity and its structure is extremely simple compared to that of the reciprocating compressor. Consequently suction pressure loss is minor. However, the pressure pulsation is present and the indicated loss caused by it cannot be ignored in some cases of the designs of pipeline system and of running conditions. As for the flow in the pipeline, the following equations are derived by making

use of the equation of continuity, the law of conservation of momentum and the law of conservation of energy, if one-dimensional compressive flow is assumed.

$$\left. \begin{array}{l} \frac{\partial \rho}{\partial t} + \rho \frac{\partial u}{\partial x} + u \frac{\partial \rho}{\partial x} = 0 \\ \frac{\partial u}{\partial t} + u \frac{\partial u}{\partial x} + \frac{1}{\rho} \frac{\partial p}{\partial x} + \frac{4f}{D} \frac{u^2}{2} \frac{u}{|u|} = 0 \\ \frac{\partial E}{\partial t} + u \frac{\partial E}{\partial x} + \frac{1}{\rho} \frac{\partial (\rho u)}{\partial x} = 0 \end{array} \right\} \quad (2)$$

where

- x : Coordinate in longitudinal direction of pipeline
- t : Time
- ρ : Density
- p : Pressure
- u : Flow velocity
- f : Tube friction coefficient
- D : Suction tube diameter
- E : $RgT/(\kappa-1) + u^2/2$
- R : Gas constant
- κ : Adiabatic constant
- T : Temperature

The pressure pulsation is analyzed by solving these equations with the equation of state and the boundary conditions at both ends of the suction pipeline system taken into account using modified FLIC (Fluid In Cell) method (1).

(3) Discharge pressure loss ... For evaluation of the discharge indicated loss, the pressure pulsation is taken into account in the same manner as the analysis for the suction system.

(4) Heat input ... The estimation is made by temperature distribution analysis using our computer code by the FEM method, for the longitudinal section and the cross section of the compressor.

(5) Top clearance ... The calculation of top clearance loss varies depending on whether or not the reverse flow to the suction tube is allowed during the expansion process of the high pressure gas in the top clearance into the suction chamber. The following equation is obtained when ideal gas is assumed (2).

$$\Delta\eta_{top} = \begin{cases} \lambda(\Pi_0^{\frac{\kappa-1}{\kappa}} - 1) & \text{: With reverse flow} \\ 0 & \text{: Without reverse flow} \end{cases} \quad (3)$$

$$\frac{\Delta H_{top}}{H_0} = \begin{cases} \lambda \left[1 - \frac{\Pi - 1}{\frac{\kappa}{\kappa-1} (\Pi^{\frac{\kappa-1}{\kappa}} - 1)} \right] & \text{: With reverse flow} \\ \frac{\Pi_0 \cdot (1+\lambda) \left\{ \frac{\kappa}{\kappa-1} (\Pi^{\frac{\kappa-1}{\kappa}} - 1) + 1 \right\} - (1+\Pi_0\lambda)}{\frac{\kappa}{\kappa-1} (\Pi_0^{\frac{\kappa-1}{\kappa}})} & \text{: Without reverse flow} \end{cases} \quad (4)$$

where,

$$\Pi = \Pi_0 \{ (1 + \Pi_0 \lambda) / (1 + \lambda) \}^k$$

Π_0 : Running pressure ratio

λ : Top clearance volume ratio

H_0 : Theoretical adiabatic compression power when $\eta_v = 100\%$

ΔH_{top} : Indicated power loss due to top clearance

$\Delta \eta_{vtop}$: Drop in volumetric efficiency due to top clearance

With or without reverse flow is affected by the form and the position of the port.

Mechanical Loss

(1) Bearings ... Each bearing is a dynamically loaded bearing, the acting load of which varies in accordance with the change in the gas pressure in the cylinder. If it is assumed that the bearings are subject to the mean static load and are under fluid lubrication, the bearing loss is expressed by the following equation.

$$H = fWU \quad (5)$$

Friction coefficient f is defined as follows (3).

$$f\psi^{-1} = 2\pi^2 S + \Delta f\psi^{-1} \quad (6)$$

where,

W: Bearing load

U: Shaft linear velocity

ψ : Bearing clearance ratio

Δf : Correction of friction coefficient

S: Sommerfeld number

When more accurate treatment is required, the numerical analysis by the finite length journal bearing theory subject to dynamic load is used.

(2) Inclined bearing characteristics ... Ideally speaking, the bearing should operate under the fluid lubrication, but in the rotary compressor, it is considered that the bearing operates usually under the boundary lubrication. Because the bearings of a rotary compressor have a small diameter, and the diametral clearance is 10-20 μm , therefore the minimum oil film thickness (h_{min}) during operation will be the order of several μm . On the other hand, the sum of the surface roughness of the shaft and bearing (ΣR_{max}) is also of the same order. Moreover, the shaft is apt to incline in the bearing because of its insufficient rigidity.

Therefore, we analyzed the working condition of the bearing when it inclined, assuming that the bearings are subject to

the mean static load. Although the bearings are subject to the dynamical load in real compressor, it is considered that the mean static treatment could explain the real operating condition considerably.

Fig. 2 indicates the relationship between the load operating position and the shaft deflection. The — line shows inclined coefficient Li/c (which represents shaft deflection) when the load works on the X point. The bearing radial clearance is denoted by C and the material of shaft is denoted by α and β . (Young's modulus of β is greater than that of α .) The --- line shows the load working points which were calculated from the oil pressure distribution when the bearing inclined. The cross points of the — and the --- line show

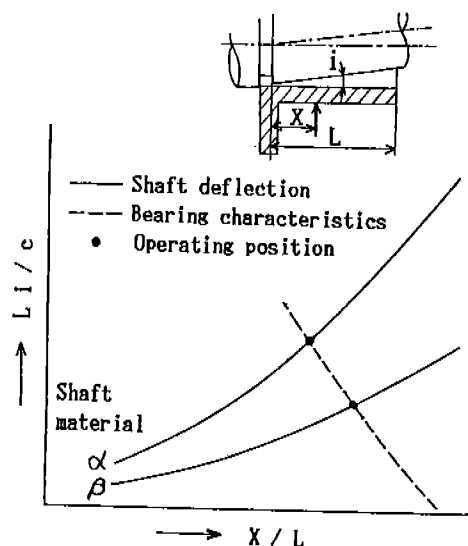


Fig. 2 Shaft Deflection and Bearing Characteristics

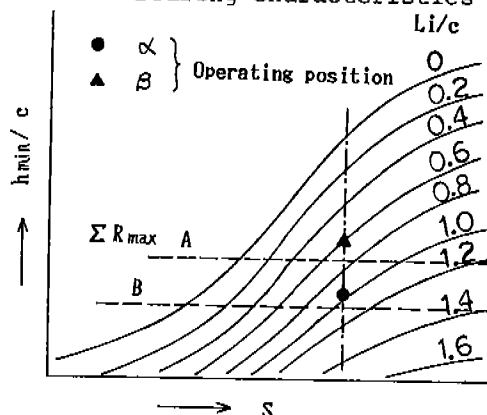


Fig. 3 Inclined Bearing Characteristics

the center of the load operating positions and the shaft deflection of given bearings. Then we plotted these operating positions on the curves of the relationship between S and h_{min}/c as shown in Fig. 3.

In Fig. 3, the --- line which is parallel to the axis of abscissa shows the points which h_{min} is equal to ΣR_{max} (It's value is denoted by A or B and $A > B$). If the operating position of the bearing is upper side of this --- line, oil film in the bearing is thicker than the sum of the surface roughness (ΣR_{max}), therefore the bearing operates under the fluid lubrication.

It is clear from Fig. 3 that the smaller the ΣR_{max} and the greater the Young's modulus, the bearing is apt to operate under the fluid lubrication.

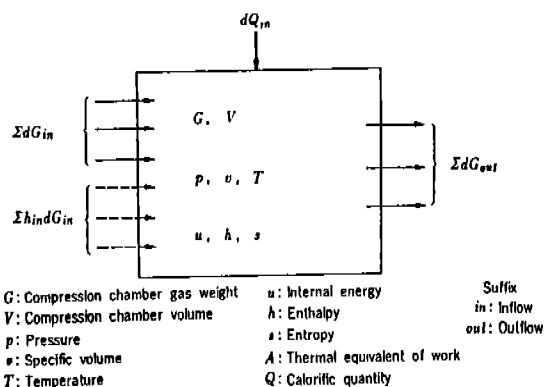
(3) Blade ... The load to the blade produced by the gas pressure and sliding speed can be easily obtained, and assuming the coefficient of friction between the blade and the cylinder is given, the mechanical loss of the blade can be easily calculated. The mechanical loss at the blade tip can also be calculated in the same manner if the friction coefficient is given. These friction coefficients were obtained through sliding model tests (7).

Motor Loss

The motor loss is evaluated by making use of the efficiency curve. The efficiency curve is obtained after the motor temperature is elevated to the same temperature as used in the compressor, by measuring the torque input to the motor.

PERFORMANCE ANALYSIS COMPUTER PROGRAM

Based on the technique for calculation of the loss indicated before, we have developed a computer program for calculating



the performance of a rotary compressor using real refrigerant gas characteristics. The prime objective of this program is to evaluate the effect of the internal leakage on the performance, which is peculiar to rotary compressors. In this program the calculations of the mechanical loss, the pressure loss, etc. are included, and it is also possible to evaluate the influence of gas heating by giving the heat input value. The outline of this program is as follows.

For the system shown in Fig. 4, with respect to the pressure P , the temperature T and the weight G of the gas in the compression chamber, the following equations are obtained when the first law of thermodynamics, the law of conservation of mass and general thermodynamic relations are used.

$$\frac{dT}{d\phi} = \frac{1}{G \left(\frac{\partial u}{\partial T} \right)} \left[\frac{dQ_{in}}{d\phi} - \left\{ \left(\frac{\partial u}{\partial v} \right)_T + Ap \right\} dV/d\phi + \left\{ \left(\frac{\partial u}{\partial v} \right)_T + Ap \right\} v \left(\Sigma \frac{dG_{in}}{d\phi} - \Sigma \frac{dG_{out}}{d\phi} \right) + \Sigma (h_{in} - h) \frac{dG_{in}}{d\phi} \right] \quad (7)$$

$$\frac{dG}{d\phi} = \Sigma \frac{dG_{in}}{d\phi} - \Sigma \frac{dG_{out}}{d\phi} \quad (8)$$

If the dimensions and operating conditions of the compressor are given, the displacement and its derivative at each shaft rotating angle, leakage $dG_{in}/d\phi$, $dG_{out}/d\phi$ and external heat input $dQ_{in}/d\phi$ and various thermodynamic variables in Eq. (7) can be calculated. The gas state value in the next step is obtained by performing numerical integration of the right hand sides of Eq. (7) and (8). The calculation is iterated until they are converged over a stroke of the compressor.

A comparison between the measured values and the calculation results using this program is given in Fig. 5. It is seen that the calculation results coincide well with the measured values and that this program is useful for evaluating the performance. As for the suction and discharge strokes, the calculation is made by treating them as pulsating flows, which is not reported here.

INTERNAL MEASUREMENT

In order to evaluate each loss of the compressor stated above and to examine the counter-measures for reducing such losses, a test compressor having a flanged housing that permits easy disassembly/reassembly, was produced, and a test was conducted mainly to check the indicated loss of the compressor.

The pV diagram shown by the — line in Fig. 5 was obtained from the measured wave-form by using data processing apparatus. The — line in this figure indicates an ideal state without the loss. It is possible to observe the levels of the various indicated loss from these lines. The — line in the figure indicates the calculation results using the performance analysis program described before. Both agreed well with each other.

MODEL TESTS

Fig. 7 gives typical comparison between the measurement results obtained using

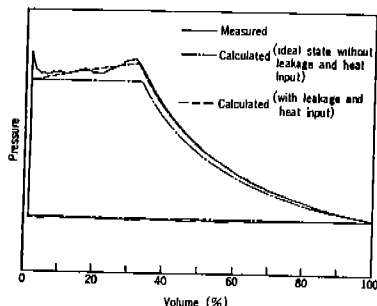


Fig. 5 pV Diagram - Measured Data Compared with Calculated Results

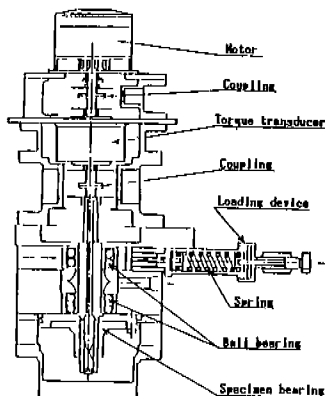


Fig. 6 Test Apparatus for Bearing Characteristics

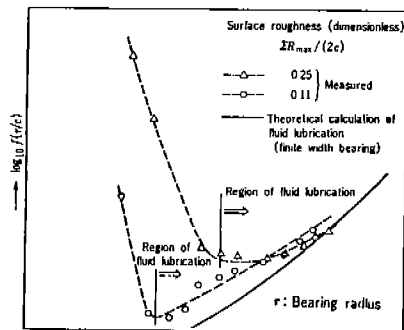


Fig. 7 Bearing Frictional Characteristics

the test apparatus shown in Fig. 6 and the calculated values of bearing friction characteristics. As mentioned before, depending on the design, it is considered that the bearing operates usually in the boundary lubrication region instead of fluid lubrication region. In this case, the friction coefficient is, as shown in Fig. 7, large and the power loss increases, which results the efficiency drop.

Fig. 9 indicates the typical results of an analysis and a test of the two-phase flow leakage characteristics in a small clearance using the test apparatus shown in Fig. 8. It is indicated that the larger the oil flow rate is, the smaller the gas leakage flow rate becomes. The oil that leaked through clearances is present in the cylinder volume. It is considered that the relation between the amount of this leaked oil and the sizes of the clearances

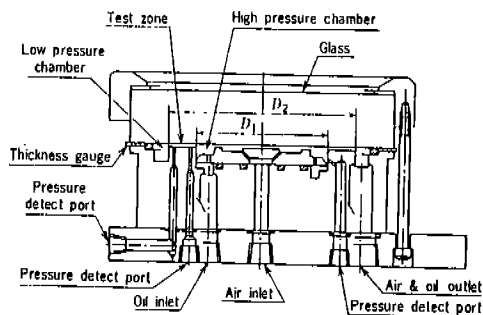


Fig. 8 Test Apparatus of Leakage Characteristics in Two-phase Flow.

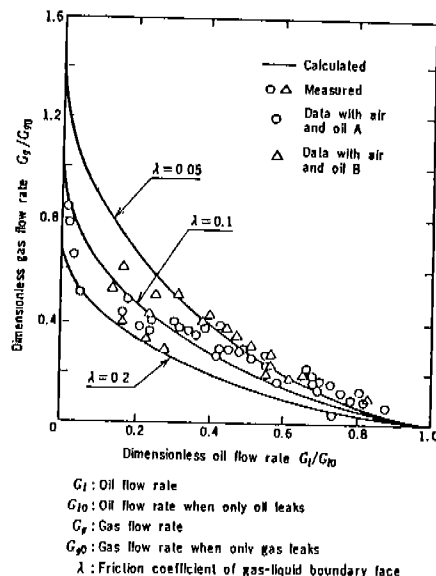


Fig. 9 Leakage Characteristics in Two-phase Flow through Narrow Clearance

determines the type of the leakage flow, i.e., a single-phase flow of the oil, or a two-phase flow of the oil and gas mixture. When the latter type of the leakage flow occurs the decrease in the performance of the compressor is large compared with the former type because the gas leakage increases. As the oil volume in the cylinder varies by the selection of clearances at various points, there is an optimum value of each clearance for the reduction of leakage.

RESULTS OF LOSS ANALYSIS

The loss in the compressor was analyzed by making use of the performance analysis techniques and the results of various tests, which are described before. A break-down of the power consumption of our compressor of conventional type is shown in Table 1. Of the power consumption, 43% is due to the various power losses. The largest power loss is the motor loss which accounts for about one half of the total power loss. The indicated and the mechanical losses follow. It is also learned that the mechanical loss, the leakage loss, the suction and discharge indicated losses and the gas superheat indicated loss are about 10-15% of the total power loss and that they are roughly of the same level.

Table 1 Power Loss in Rotary Compressor before Improvement

Item	Breakdown	Power consumption **	Breakdown of power loss
Total power consumption *		100	—
Theoretical adiabatic compression power		57.2	—
Power loss		42.8	100 %
Motor loss		20.5	48.0%
Mechanical loss		6.0	14.0%
Indicated loss		16.3	38.0%
Leakage		5.0	11.7%
Suction/discharge pressure loss		5.7	13.3%
Top clearance		1.6	3.6%
Gas superheating		4.0	9.4%
Overall efficiency		57.2%	—

* (compressor input)

** (total power consumption = 100)

COUNTER-MEASURES FOR THE REDUCTION OF LOSSES AND THEIR EVALUATION

Judging from the loss analysis described before, the counter-measures were planned for reducing the loss as indicated in Table 2. The confirmation tests on the effectiveness of these measures were also conducted. Then the counter-measures which have the large effects for the performance improvement were selected and were applied to real machines.

Table 2 Measures for Loss Reduction

Loss item	Concrete measure for reduction
Leakage	Leak clearances were reduced to the optimum keeping gas sealing by oil
Pressure loss	Suction: Suction tube diameter was increased Discharge: (1) Discharge port form was changed (cylinder notch angle) (2) Discharge muffler position was changed
Top clearance	Reduction of top clearance volume (reduction of plate thickness at discharge valve)
Friction	Improvement of surface roughness
Motor	Improvement of efficiency through matching of load with motor torque and improvement of slot fulness

Fig. 10 shows the effect of the axial clearances at the rotor's top and bottom end faces to the compressor PV diagram. The reduction of the indicated loss caused by the reduction of the leakage is clearly indicated in the diagram.

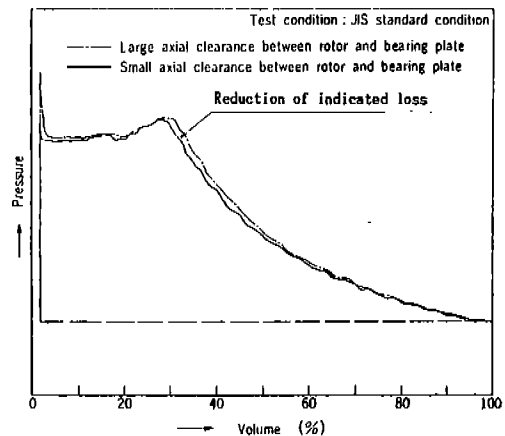


Fig. 10 Effect of Axial Clearance between Rotor and Bearing Plate (Measured)

Fig. 11 indicates the calculated values of the reduction of the suction indicated loss caused by a change in the suction tube diameter. Fig. 12 indicates the typical measurements of the pressure pulsation in the suction chamber. This figure shows the effect of the suction tube diameter. It is

possible to reduce the indicated loss by changing the suction tube diameter. In Fig. 12, the calculated values are also shown.

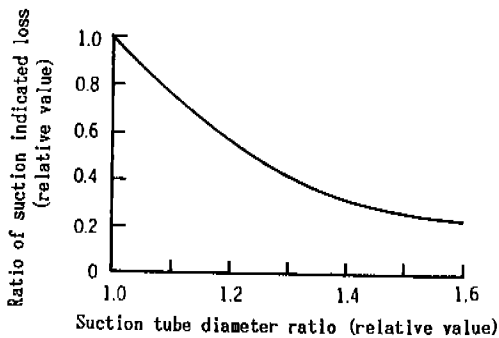


Fig. 11 Relation between Suction Indicated Loss and Suction Tube Diameter.

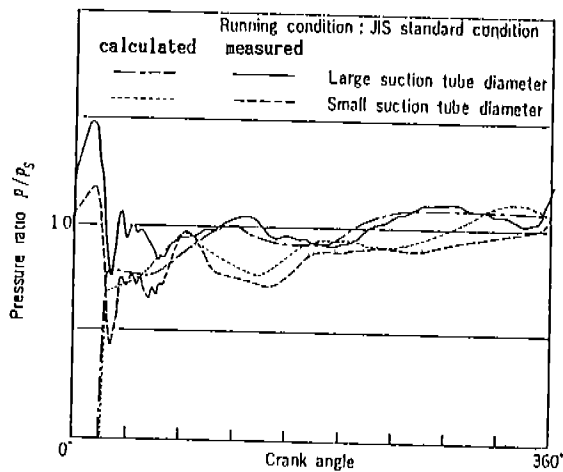


Fig. 12 Effect of Suction Tube Diameter on Gas Pressure Pulsation in Suction Process Cylinder

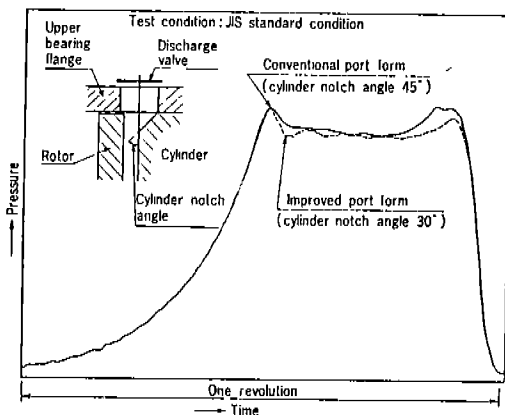


Fig. 13 Effect of Discharge Port Shape (Measured)

Fig. 13 indicates how the cylinder pressure is influenced when the modification in the form of the passage of the discharge port is made. It is observed that the reduction of the discharge indicated loss can be obtained by this modification.

The motor loss is the largest among the power losses. To reduce the motor loss, the improvement of the efficiency was attempted through optimization of the matching between the compressor load and motor torque, and also through reduction of copper loss by improving the ratio of the coil's sectional area to the slot's sectional area, that is, slot fullness.

The improvement measures which were planned and experimentally confirmed as described above were incorporated in the high efficiency rotary compressors. The results of the analysis of the breakdown of power consumption of improved rotary compressor are shown in Table 3. Each loss is reduced, and it is seen that the reduction in the motor loss and the indicated losses of the leakage, discharge, suction pressure and top clearance are particularly large. It is also learned that the total efficiency was improved by about 12%, that is, from 57.2% of conventional type shown in Table 1 to 64.1% shown in Table 3.

Table 3 Power Loss in the Improved Rotary Compressor

Item	Breakdown	Power consumption **	Ratio of losses **
Total power consumption *		89.3	89.3%
Theoretical adiabatic compression power		57.2	100.0%
Power loss		32.1	78.3%
Motor loss		15.5	79.0%
Mechanical loss		5.1	88.3%
Indicated loss		11.5	73.0%
Leakage		3.0	64.0%
Suction/discharge pressure loss		3.7	66.7%
Top clearance		1.1	73.3%
Gas superheating		3.7	95.0%
Overall efficiency		64.1%	—

*(compressor input)

** (total power consumption of conventional type = 100)

*** (each item of losses in the conventional type = 100%)

CAPACITY CONTROL

The efficiency of a compressor decrease generally, when the capacity is modulated and the efficiency more largely drops when the amount of capacity control increases (5). With a conventional compressor the efficiency drop at the 33% capacity control operation (during the operation with a 67% load) was 10% or more of the full load. With the newly developed compressor, however, even if capacity control is made to such a major extent as 33%, the efficiency drop is suppressed only to 6% of the full load and thus the improvement in the efficiency during the capacity control is also accomplished.

Mechanism of the capacity control is shown in Fig. 14. A release hole is made in the lower bearing. During partial load operation, the bypass pipe is connected to the low pressure side, and as a result, the release valve is opened and the capacity is reduced by releasing the gas in the compression process to the

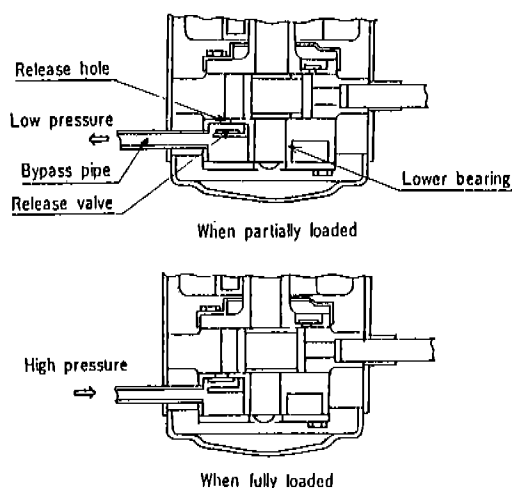


Fig. 14 Mechanism of Compressor Capacity Control

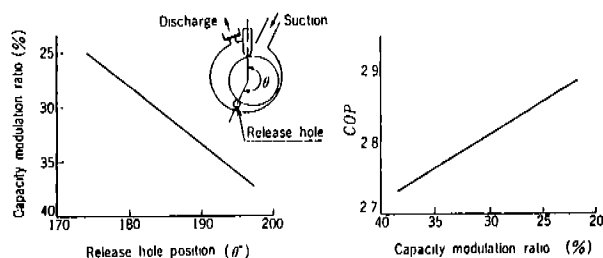


Fig. 15 Characteristics of Capacity Control

low pressure side until the release hole is plugged by the rotor, while during full load operation the by-pass pipe is connected with the high pressure side, the release valve is closed by the high pressure and the usual compressing operation is performed.

The location of the release hole was determined from the relation between the release hole position and performance shown in Fig. 15 so that the capacity control ratio becomes 33%, which is optimum for a room air-conditioner.

CONCLUSION

In order to meet the needs for energy saving of room air-conditioners, the studies for improving the efficiency of compressors were carried out. The analysis of the losses in the compressor and the evaluation of the counter-measures to reduce them were conducted through various measurements and calculations.

As a result, the higher efficiency compressor has been developed, the performance of which is improved by 12% compared with our conventional rotary compressors. Marketing of the room air-conditioners equipped with this developed compressor started in the fall of 1982. Improvements of performance are largely dependent on technological progress and we intend to pay further attention to the energy conservation by accumulating fundamental studies on compressors in the future.

REFERENCES

- (1) Mitsubishi Juko Giho, Vol. 12, No. 5 (1975), P1
- (2) Yanagisawa, Shimizu, Preprint of JSME No. 814-9 (November, 1981), P.31
- (3) Handbook for Mechanical Engineers (6th edition), Vol. 7
- (4) H. W. Hahn, SAE Congress (July, 1966)
- (5) Fukazawa & Ozawa, Proceedings of the 1980 Purdue Compressor Technology Conference (July, 1980)
- (6) Yoshida, Takeshita, Iida, Preprint of JSME, No. 835-5 (March, 1983), P. 44
- (7) Mitsubishi Juko Giho, Vol. 18, No. 1 (1981), P. 127